SUPPLEMENTAL METHODS

Regulatory T cell Immunosuppression Potential

We evaluate Treg immunosuppressive function as previously described[1]. Briefly, PBMC were selectively depleted from $CD25^{hi}$ Treg using a limiting amount of anti-CD25 magnetic microbeads (Miltenyi Biotec) A control condition was run in parallel with PBMC flowed in the column without prior incubation with anti-CD25 microbeads. PBMC and Treg-depleted PBMC were then used in a proliferation assay as described in Material and Methods section.

RNA-seq Experiment

Sequencing

For each T-cell sample, RNA was extracted using RNeasy Micro kit (Qiagen). Libraries were prepared using the SMARTer® Stranded Total RNA-Seq Kit V2 - Pico Input Mammalian kit (Clontech Laboratories) following manufacturer protocols. Briefly, total RNA served as template for randomly primed cDNA synthesis and subsequent adapter/barcode addition. A cleavage step was then used (with ZapR) to deplete the amplified ribosomal cDNA sequences using mammalian-specific probes that hybridize to rRNA sequences. A final round of PCR enriched for non-rRNA fragments. The process was completed by Paired-End 75 bases massive parallel sequencing on Illumina HiSeq4000. RNA-seq libraries generated more than 34 million reads per sample with >93% of sequences achieving > Q30 Phred quality scores.

RNAseq analysis

Raw sequencing data were checked and visualized for quality using FastQC (v0.11.5). The RNAseq reads were aligned to the reference genome GRCh38 release 90 using STAR (v2.5). Read summarization and gene counts were performed using the featureCounts function from the Subread package (v1.4.6). Data normalization and differential gene expression were performed with the DESeq2 R package (v1.26.0). The DESeq2 HTS pre-filtering step filtered in 13471 ENSG identifiers (corresponding to 12270 unique HGNC gene symbols) from the 58243 ENSG identifiers of the raw counts. Significant genes were defined as $p < .05$ after adjustment for False Discovery Rate (FDR) correction and used for downstream analysis. PCA was displayed using the factoextra R package (v1.23) (v1.0.7) on HTS Filtered data normalized by variance stabilizing transformation from the DESeq2 package.

Biological interpretation

Gene set enrichment analysis (GSEA) was used to identify the predefined gene sets that were enriched at Day 7 or Day 0 in each T-cell subset. The gene sets corresponded to canonical pathways (C2.CP) from GSEA MSigDb database version 7.1. GSEA preRanked analysis was conducted on the ranked gene lists generated for each pairwise comparison between D7 and D0 for each T-cell subset, the ranking being applied on the statistics of the Wald test (DESeq2 R package). Both the Reactome and Kegg databases organize canonical pathways into hierarchies of classes and subclasses. For each GSEA analysis, significant pathways were filtered in, a pathway being considered significant for FDR q-value <.05. Venn diagram indicates the number of Reactome pathways in common or specific to each T-cell subset. Pie charts display the percentage of differentially expressed Reactome pathways grouped under their uppermost hierarchical levels. Significant pathways from the Reactome database related to "Cell Cycle", "DNA Replication", "Immune System", "Metabolism", and "Signaling Transduction", as well as those from Kegg database related to "Cell Motility", "Signaling Molecules and Interaction" and "Circulatory System" were displayed as dot plots for CD4 PD-1^+ and CD8 PD-1^+ subsets. The GeneRatio corresponded to the number of genes of a specific pathway present in the dataset after HTS Filtering divided by the total number of genes in this pathway.

Hierarchical Cluster Analysis (HCA)

Agglomerative hierarchical clustering was performed on the percentages of CD4, CD8, and Treg populations using the Pearson's correlation for samples, Euclidean distance for the variables as metric criteria, and Ward's method as the linkage criteria.

Supplemental statistical methods

PFS was measured from the date of inclusion to the date of last follow-up or progression, relapse, or death. Survival differences were assessed using the log-rank test considering events having occurred before the end of maintenance treatment (i.e. 18 months).

Supplemental References

1. Menard C, Ghiringhelli F, Roux S, et al. Ctla-4 blockade confers lymphocyte resistance to regulatory T-cells in advanced melanoma: surrogate marker of efficacy of tremelimumab? *Clin Cancer Res*. 2008;14(16):5242-5249.

Supplemental Table 1. Characteristics of patients enrolled in the immune monitoring study

	FL Cohort without flow cytometry data (n=59)	FL Cohort with flow cytometry data (n=27)	Test, P-value
Age (years)			
Median (IQR)	67.0 (58.0-72.5)	59.4 (51.0-67.0)	.025
Range	39.0-87.0	39.0-83.0	
Sex			
Male	38 (64.4%)	16 (59.3%)	.647
Female	21 (35.6%)	11 (40.7%)	
Number of previous therapies			
Mean (SD)	2.2 (1.6)	1.8 (1.0)	.469
Median (IQR)	2.0 (1.0-3.0)	1.0 (1.0-2.5)	
Range	1.0-7.0	1.0-5.0	
Type of relapse			
Early progression of disease (within 24 months of initial diagnosis)	17 (28.8%)	7 (25.9%)	.782
Late progression	42 (71.2%)	20 (74.1%)	
Refractory to a Rituximab-containing regimen			
No	47 (79.7%)	19 (70.4%)	.344
Yes	12 (20.3%)	8 (29.6%)	
Refractory to previous lymphoma therapy			
No	49 (83.1%)	22 (81.5%)	.859
Yes	10 (16.9%)	5 (18.5%)	
Ann Arbor Stage			
I-II	9 (15.3%)	5 (18.5%)	.704
III-IV	50 (84.7%)	22 (81.5%)	
Performance Status (ECOG)			
0-1	56 (94.9%)	27 (100.0%)	NA
2	3 (5.1%)	0 (0.0%)	
Bone marrow involvement			
Missing	6	1	
No	37 (69.8%)	17 (65.4%)	.681
Yes	14 (26.4%)	8 (30.8%)	
LDH (IU/L)			
Missing	1	1	
Normal	41 (70.7%)	17 (65.4%)	.627
More than upper limit of normal	17 (29.3%)	9 (34.6%)	
B-symptoms			
No	49 (83.1%)	23 (85.2%)	1
Yes	10 (16.9%)	4 (14.8%)	
FLIPI			
Missing	1	1	
0-1	26 (44.8%)	8 (30.8%)	.255
2	21 (36.2%)	9 (34.6%)	
3-5	11 (19.0%)	9 (34.6%)	
Response Cheson 1999 at intermediate assessment after C3			
Missing	5	0	
CR, unCR	16 (29.6%)	7 (25.9%)	.854
PR	25 (46.3%)	12 (44.5%)	
PD, SD	13 (24.1%)	8 (29.6%)	
Response Cheson 1999 at the end of induction			
Missing	6	0	
CR, unCR	22 (41.5%)	11 (40.7%)	.814
PR	24 (45.3%)	11 (40.7%)	
PD, SD	7 (13.2%)	5 (18.6%)	
PFS status			
No event	37 (62.7%)	14 (51.9%)	.341
Event	22 (37.3%)	13 (48.1%)	
OS status			
No event	47 (79.7%)	22 (81.5%)	.844
Event	12 (20.3%)	5 (18.5%)	

Data are mean (SD). n (%) or median (IQR). unless otherwise stated. CR: Complete Remission; unCR: unconfirmed Complete Remission; PR: Partial Response; PD: Progressive Disease; SD: Stable Disease

Supplemental Table 2: List of the antibodies used in flow cytometry panels

Target antigen	Clone	Provider
CD3	UCHT1	Beckman-Coulter
CD4	RPA-T4	Becton-Dickinson
CD8	RPA-T8	Becton-Dickinson
CD8	BW135/80	Miltenyi Biotec
CD25	M-A251	Becton-Dickinson
CD45	HI30	Becton-Dickinson
CD45RA	T6D11	Miltenyi Biotec
CD45RA	HI100	Becton-Dickinson
CD56	B159	Becton-Dickinson
CD127	HIL-7R-M21	Becton-Dickinson
CD137	4B4-1	Becton-Dickinson
CCR7	150503	R&D Systems
CXCR5	51505	R&D Systems
FoxP3	259D/C7	Becton-Dickinson
HLA-DR	Immu-357	Beckman-Coulter
Ki-67	MIB-1	Dako
PD-1	eBioJ105	eBioscience
Tim-3	344823	R&D Systems

Supplemental Table 3. Lists of genes differentially expressed after one-week lenalidomide in PD-1^{+} and PD-1^{-} CD4 and CD8 T cells. First to fourth sheets display the respective lists of differentially expressed genes at D7 versus D0 for CD4 PD-1^{-} T cells, CD4 PD-1^{+} T cells, CD8 PD-1^{-} T cells, and CD8 PD-1^{+} T-cell subsets.

Supplemental Table 4. List of Kegg and Reactome pathways upregulated in PD-1+ T cells after one-week lenalidomide

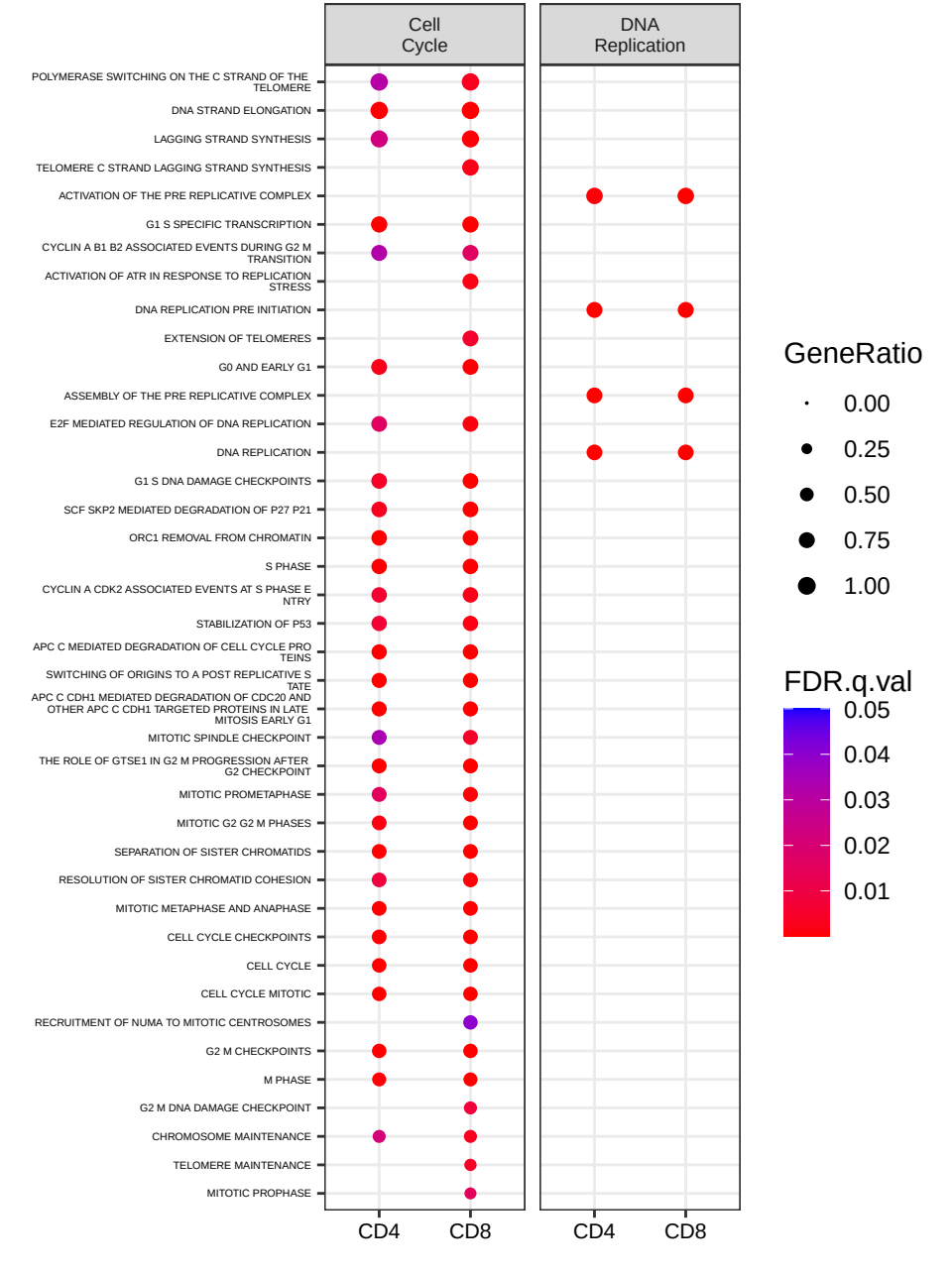

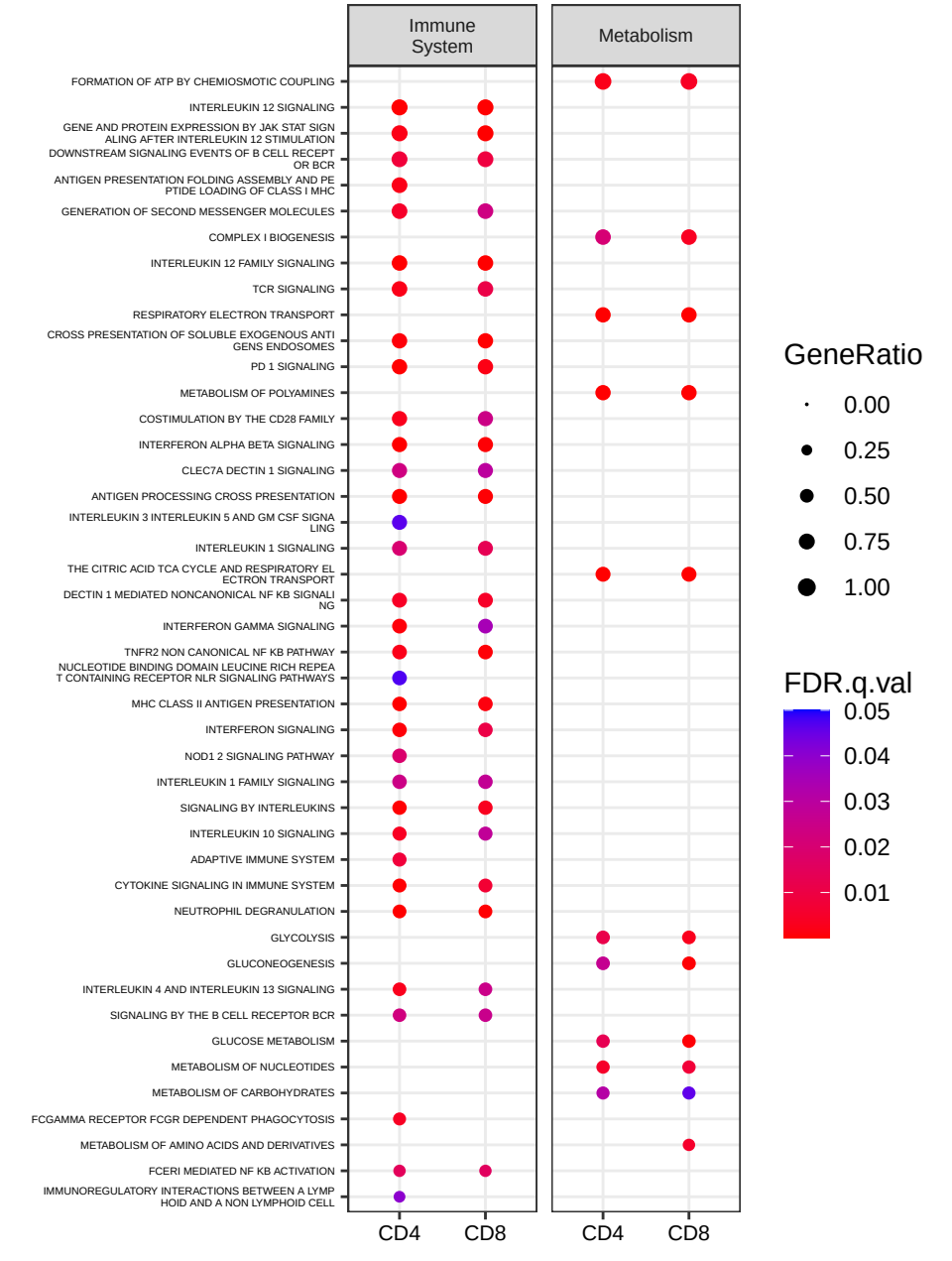
Immune System
Metabolism
FORMATION OF ATP BY CHEMIOSMOTIC COUPLING
INTERLEUKIN 12 SIGNALING
GENE AND PROTEIN EXPRESSION BY JAK STAT SIGNALING AFTER INTERLEUKIN 12 STIMULATION
DOWNSTREAM SIGNALING EVENTS OF B CELL RECEPTOR BCR
ANTIGEN PRESENTATION FOLDING ASSEMBLY AND PEPTIDE LOADING OF CLASS I MHC
GENERATION OF SECOND MESSENGER MOLECULES
COMPLEX I BIOGENESIS
INTERLEUKIN 12 FAMILY SIGNALING
TCR SIGNALING
RESPIRATORY ELECTRON TRANSPORT
CROSS PRESENTATION OF SOLUBLE EXOGENOUS ANTIGENS ENDOSOMES
PD 1 SIGNALING
METABOLISM OF POLYAMINES
COSTIMULATION BY THE CD28 FAMILY
INTERFERON ALPHA BETA SIGNALING
CLEC7A DECTIN 1 SIGNALING
ANTIGEN PROCESSING CROSS PRESENTATION
INTERLEUKIN 3 INTERLEUKIN 5 AND GM CSF SIGNALING
INTERLEUKIN 1 SIGNALING
THE CITRIC ACID TCA CYCLE AND RESPIRATORY ELECTRON TRANSPORT
DECTIN 1 MEDIATED NONCANONICAL NF KB SIGNALING
INTERFERON GAMMA SIGNALING
TNFR2 NON CANONICAL NF KB PATHWAY
NUCLEOTIDE BINDING DOMAIN LEUCINE RICH REPEAT CONTAINING RECEPTOR NLR SIGNALING PATHWAYS
MHC CLASS II ANTIGEN PRESENTATION
INTERFERON SIGNALING
NOD1 2 SIGNALING PATHWAY
INTERLEUKIN 1 FAMILY SIGNALING
SIGNALING BY INTERLEUKINS
INTERLEUKIN 10 SIGNALING
ADAPTIVE IMMUNE SYSTEM
CYTOKINE SIGNALING IN IMMUNE SYSTEM
NEUTROPHIL DEGRANULATION
GLYCOLYSIS
GLUCONEOGENESIS
INTERLEUKIN 4 AND INTERLEUKIN 13 SIGNALING
SIGNALING BY THE B CELL RECEPTOR BCR
GLUCOSE METABOLISM
METABOLISM OF NUCLEOTIDES
METABOLISM OF CARBOHYDRATES
FCGAMMA RECEPTOR FCGR DEPENDENT PHAGOCYTOSIS
METABOLISM OF AMINO ACIDS AND DERIVATIVES
FCERI MEDIATED NF KB ACTIVATION
IMMUNOREGULATORY INTERACTIONS BETWEEN A LYMPHOID AND A NON LYMPHOID CELL
CD4
CD8
CD4
CD8
GeneRatio
0.00
0.25
0.50
0.75
1.00
FDR.q.val
0.05
0.04
0.03
0.02
0.01

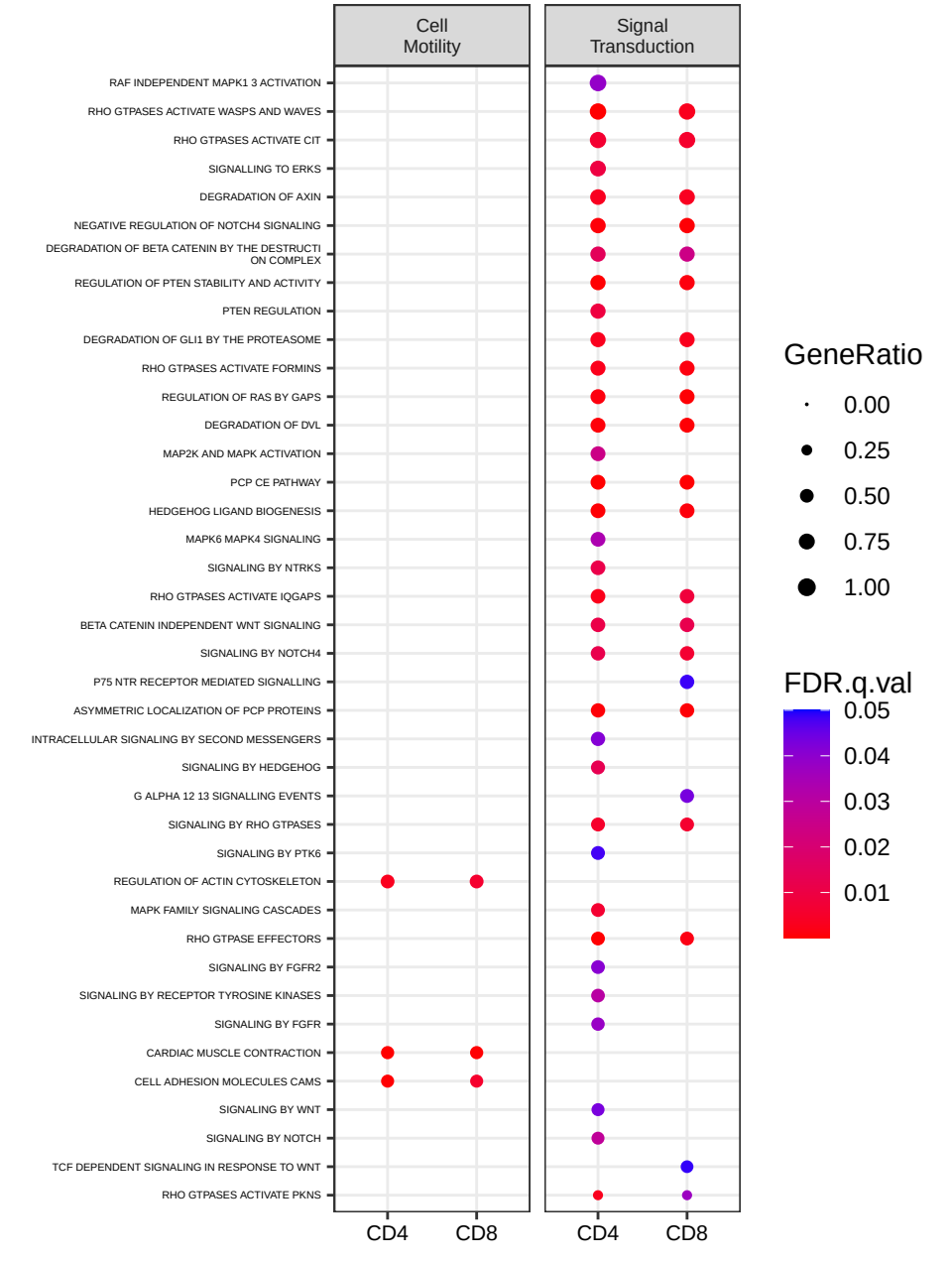
Cell Motility
Signal Transduction
RAF INDEPENDENT MAPK1 3 ACTIVATION
RHO GTPASES ACTIVATE WASPS AND WAVES
RHO GTPASES ACTIVATE CIT
SIGNALLING TO ERKS
DEGRADATION OF AXIN
NEGATIVE REGULATION OF NOTCH4 SIGNALING
DEGRADATION OF BETA CATENIN BY THE DESTRUCTI ON COMPLEX
REGULATION OF PTEN STABILITY AND ACTIVITY
PTEN REGULATION
DEGRADATION OF GLI1 BY THE PROTEASOME
RHO GTPASES ACTIVATE FORMINS
REGULATION OF RAS BY GAPS
DEGRADATION OF DVL
MAP2K AND MAPK ACTIVATION
PCP CE PATHWAY
HEDGEHOG LIGAND BIOGENESIS
MAPK6 MAPK4 SIGNALING
SIGNALING BY NTRKS
RHO GTPASES ACTIVATE IQGAPS
BETA CATENIN INDEPENDENT WNT SIGNALING
SIGNALING BY NOTCH4
P75 NTR RECEPTOR MEDIATED SIGNALLING
ASYMMETRIC LOCALIZATION OF PCP PROTEINS
INTRACELLULAR SIGNALING BY SECOND MESSENGERS
SIGNALING BY HEDGEHOG
G ALPHA 12 13 SIGNALLING EVENTS
SIGNALING BY RHO GTPASES
SIGNALING BY PTK6
REGULATION OF ACTIN CYTOSKELETON
MAPK FAMILY SIGNALING CASCADES
RHO GTPASE EFFECTORS
SIGNALING BY FGFR2
SIGNALING BY RECEPTOR TYROSINE KINASES
SIGNALING BY FGFR
CARDIAC MUSCLE CONTRACTION
CELL ADHESION MOLECULES CAMS
SIGNALING BY WNT
SIGNALING BY NOTCH
TCF DEPENDENT SIGNALING IN RESPONSE TO WNT
RHO GTPASES ACTIVATE PKNS
CD4
CD8
CD4
CD8
GeneRatio
0.00
0.25
0.50
0.75
1.00
FDR.q.val
0.05
0.04
0.03
0.02
0.01

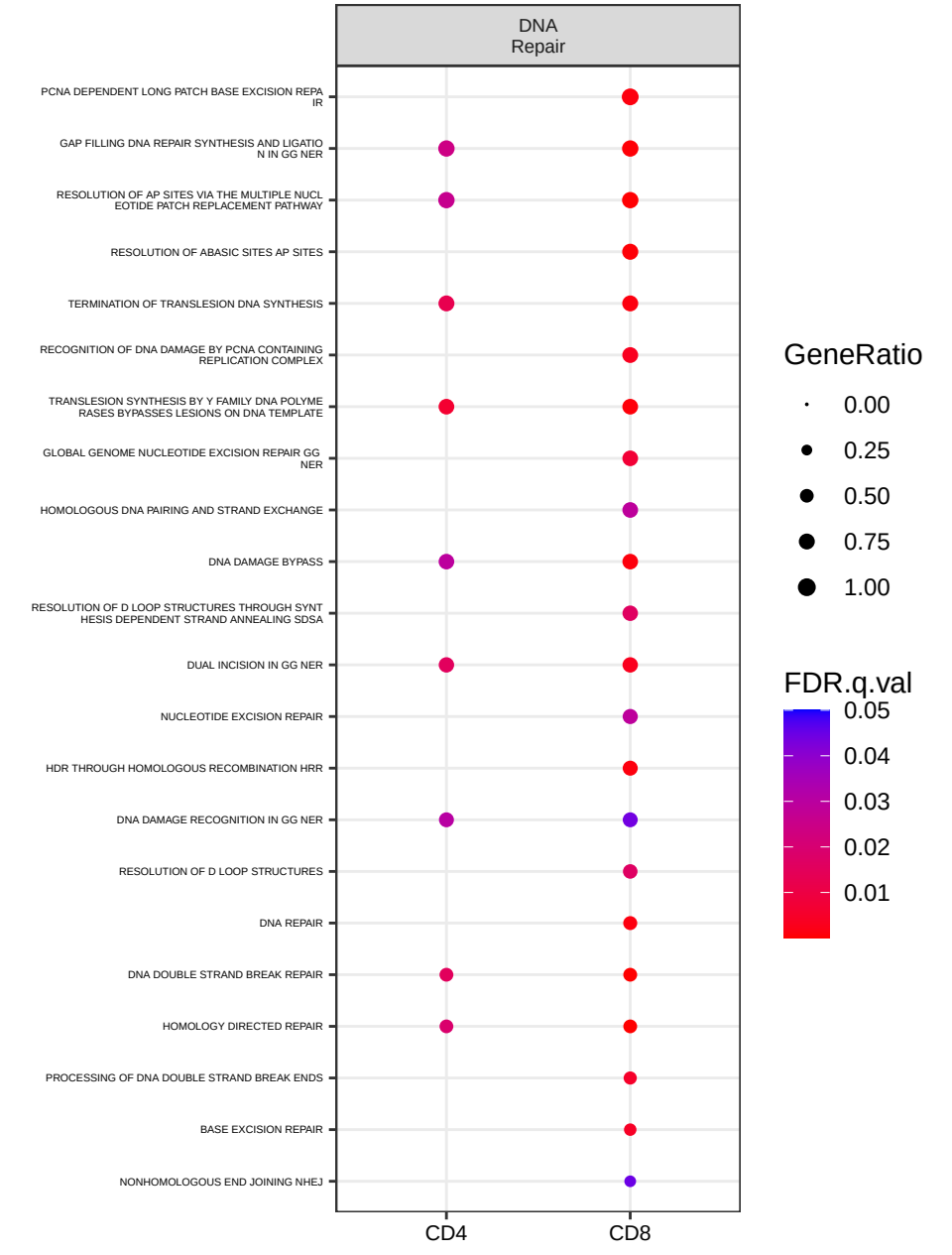
DNA
Repair
PCNA DEPENDENT LONG PATCH BASE EXCISION REPAIR
GAP FILLING DNA REPAIR SYNTHESIS AND LIGATION IN GG NER
RESOLUTION OF AP SITES VIA THE MULTIPLE NUCLEOTIDE PATCH REPLACEMENT PATHWAY
RESOLUTION OF ABASIC SITES AP SITES
TERMINATION OF TRANSLESION DNA SYNTHESIS
RECOGNITION OF DNA DAMAGE BY PCNA CONTAINING REPLICATION COMPLEX
TRANSLESION SYNTHESIS BY Y FAMILY DNA POLYMERASES BYPASSES LESIONS ON DNA TEMPLATE
GLOBAL GENOME NUCLEOTIDE EXCISION REPAIR GG NER
HOMOLOGOUS DNA PAIRING AND STRAND EXCHANGE
DNA DAMAGE BYPASS
RESOLUTION OF D LOOP STRUCTURES THROUGH SYNTHESIS DEPENDENT STRAND ANNEALING SDSA
DUAL INCISION IN GG NER
NUCLEOTIDE EXCISION REPAIR
HDR THROUGH HOMOLOGOUS RECOMBINATION HRR
DNA DAMAGE RECOGNITION IN GG NER
RESOLUTION OF D LOOP STRUCTURES
DNA REPAIR
DNA DOUBLE STRAND BREAK REPAIR
HOMOLOGY DIRECTED REPAIR
PROCESSING OF DNA DOUBLE STRAND BREAK ENDS
BASE EXCISION REPAIR
NONHOMOLOGOUS END JOINING NHEJ
CD4
CD8
GeneRatio
0.00
0.25
0.50
0.75
1.00
FDR.q.val
0.05
0.04
0.03
0.02
0.01

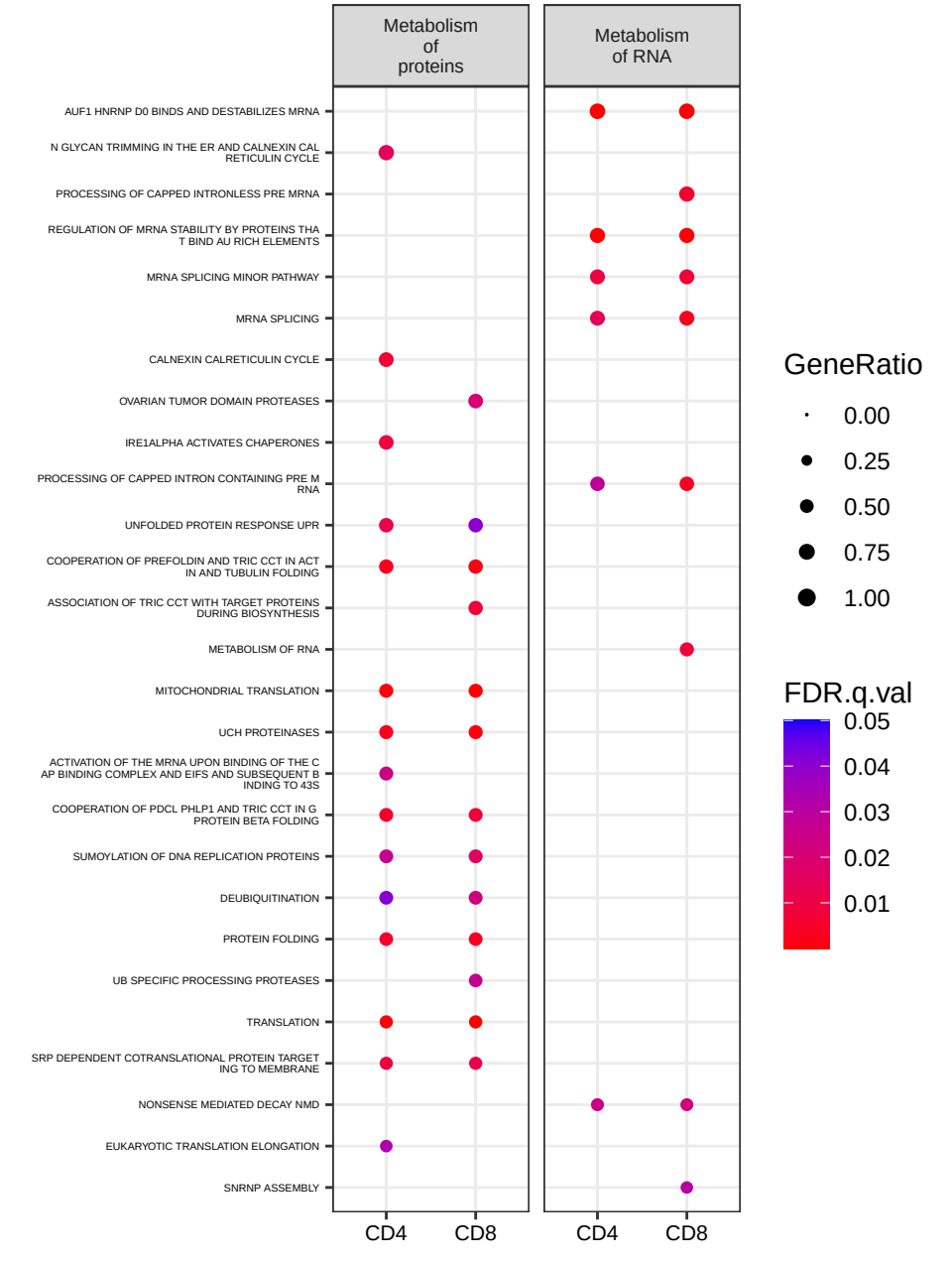
Metabolism of proteins
Metabolism of RNA
AUF1 HNRNP D0 BINDS AND DESTABILIZES MRNA
N GLYCAN TRIMMING IN THE ER AND CALNEXIN CAL RETICULIN CYCLE
PROCESSING OF CAPPED INTRONLESS PRE MRNA
REGULATION OF MRNA STABILITY BY PROTEINS THA T BIND AU RICH ELEMENTS
MRNA SPLICING MINOR PATHWAY
MRNA SPLICING
CALNEXIN CALRETICULIN CYCLE
OVARIAN TUMOR DOMAIN PROTEASES
IRE1ALPHA ACTIVATES CHAPERONES
PROCESSING OF CAPPED INTRON CONTAINING PRE M RNA
UNFOLDED PROTEIN RESPONSE UPR
COOPERATION OF PREFOLDIN AND TRIC CCT IN ACT IN AND TUBULIN FOLDING
ASSOCIATION OF TRIC CCT WITH TARGET PROTEINS DURING BIOSYNTHESIS
METABOLISM OF RNA
MITOCHONDRIAL TRANSLATION
UCH PROTEINASES
ACTIVATION OF THE MRNA UPON BINDING OF THE C AP BINDING COMPLEX AND EIFS AND SUBSEQUENT B INDING TO 43S
COOPERATION OF PDCL PHLP1 AND TRIC CCT IN G PROTEIN BETA FOLDING
SUMOYLATION OF DNA REPLICATION PROTEINS
DEUBIQUITINATION
PROTEIN FOLDING
UB SPECIFIC PROCESSING PROTEASES
TRANSLATION
SRP DEPENDENT COTRANSLATIONAL PROTEIN TARGET ING TO MEMBRANE
NONSENSE MEDIATED DECAY NMD
EUKARYOTIC TRANSLATION ELONGATION
SNRNP ASSEMBLY
CD4
CD8
CD4
CD8
GeneRatio
0.00
0.25
0.50
0.75
1.00
FDR.q.val
0.05
0.04
0.03
0.02
0.01

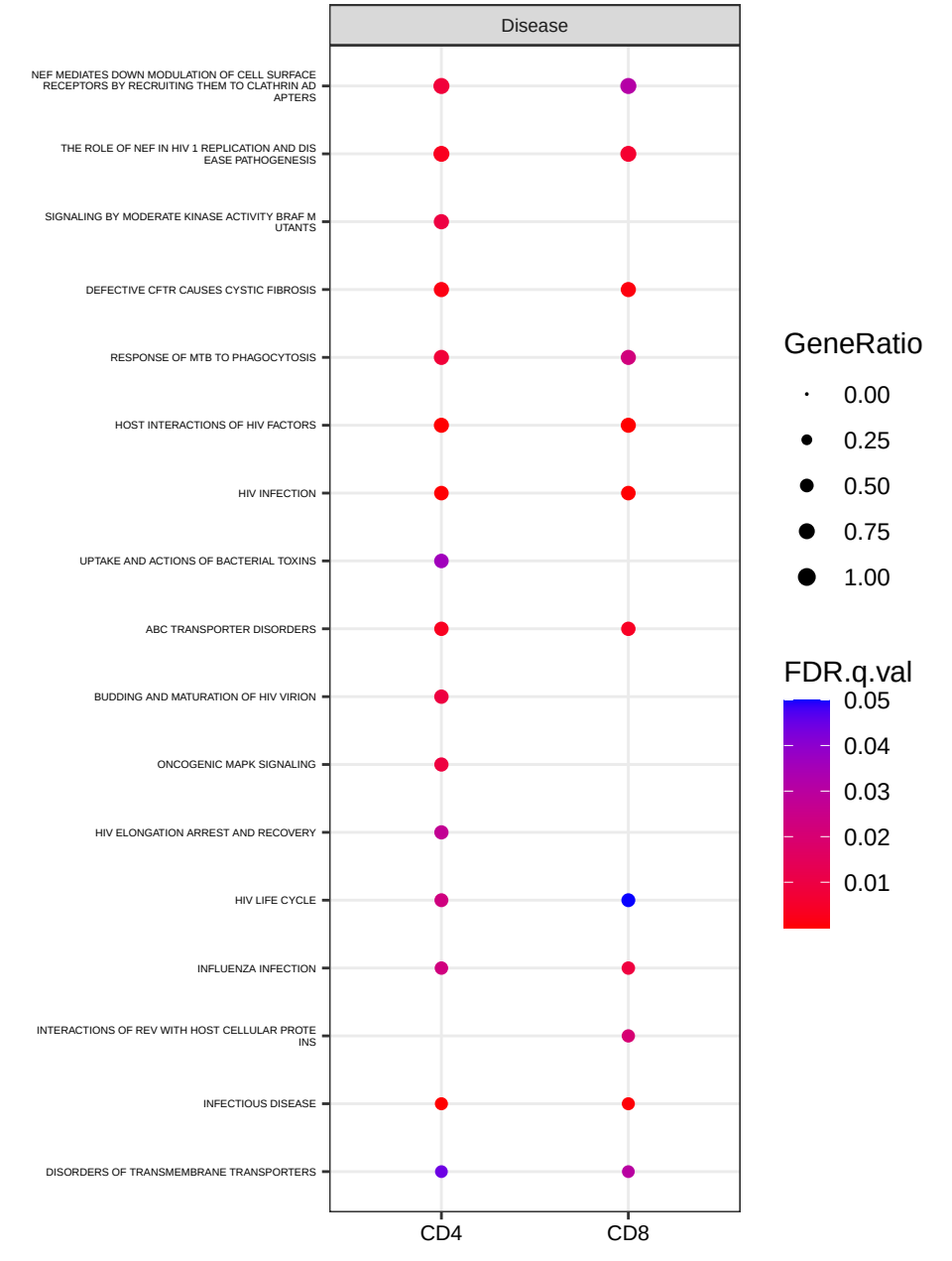
Disease
NEF MEDIATES DOWN MODULATION OF CELL SURFACE RECEPTORS BY RECRUITING THEM TO CLATHRIN ADAPTERS
THE ROLE OF NEF IN HIV 1 REPLICATION AND DISEASE PATHOGENESIS
SIGNALING BY MODERATE KINASE ACTIVITY BRAF MUTANTS
DEFECTIVE CFTR CAUSES CYSTIC FIBROSIS
RESPONSE OF MTB TO PHAGOCYTOSIS
HOST INTERACTIONS OF HIV FACTORS
HIV INFECTION
UPTAKE AND ACTIONS OF BACTERIAL TOXINS
ABC TRANSPORTER DISORDERS
BUDDING AND MATURATION OF HIV VIRION
ONCOGENIC MAPK SIGNALING
HIV ELONGATION ARREST AND RECOVERY
HIV LIFE CYCLE
INFLUENZA INFECTION
INTERACTIONS OF REV WITH HOST CELLULAR PROTEINS
INFECTIOUS DISEASE
DISORDERS OF TRANSMEMBRANE TRANSPORTERS
CD4
CD8
GeneRatio
0.00
0.25
0.50
0.75
1.00
FDR.q.val
0.05
0.04
0.03
0.02
0.01

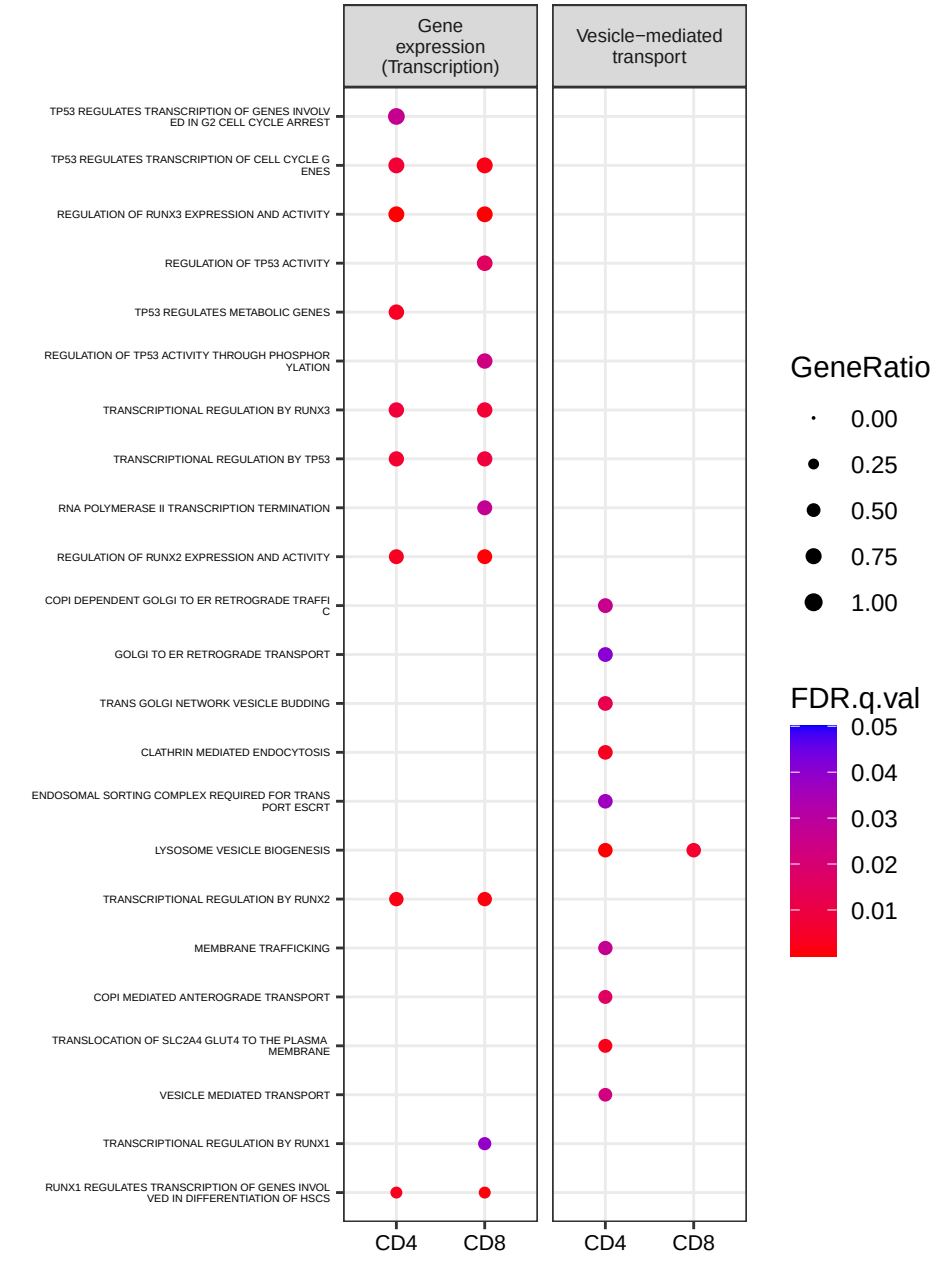
Gene expression (Transcription)
Vesicle−mediated transport
TP53 REGULATES TRANSCRIPTION OF GENES INVOLV ED IN G2 CELL CYCLE ARREST
TP53 REGULATES TRANSCRIPTION OF CELL CYCLE G ENES
REGULATION OF RUNX3 EXPRESSION AND ACTIVITY
REGULATION OF TP53 ACTIVITY
TP53 REGULATES METABOLIC GENES
REGULATION OF TP53 ACTIVITY THROUGH PHOSPHOR YLATION
TRANSCRIPTIONAL REGULATION BY RUNX3
TRANSCRIPTIONAL REGULATION BY TP53
RNA POLYMERASE II TRANSCRIPTION TERMINATION
REGULATION OF RUNX2 EXPRESSION AND ACTIVITY
COPI DEPENDENT GOLGI TO ER RETROGRADE TRAFFI C
GOLGI TO ER RETROGRADE TRANSPORT
TRANS GOLGI NETWORK VESICLE BUDDING
CLATHRIN MEDIATED ENDOCYTOSIS
ENDOSOMAL SORTING COMPLEX REQUIRED FOR TRANS PORT ESCRT
LYSOSOME VESICLE BIOGENESIS
TRANSCRIPTIONAL REGULATION BY RUNX2
MEMBRANE TRAFFICKING
COPI MEDIATED ANTEROGRADE TRANSPORT
TRANSLOCATION OF SLC2A4 GLUT4 TO THE PLASMA MEMBRANE
VESICLE MEDIATED TRANSPORT
TRANSCRIPTIONAL REGULATION BY RUNX1
RUNX1 REGULATES TRANSCRIPTION OF GENES INVOL VED IN DIFFERENTIATION OF HSCS
CD4
CD8
CD4
CD8
GeneRatio
0.00
0.25
0.50
0.75
1.00
FDR.q.val
0.05
0.04
0.03
0.02
0.01

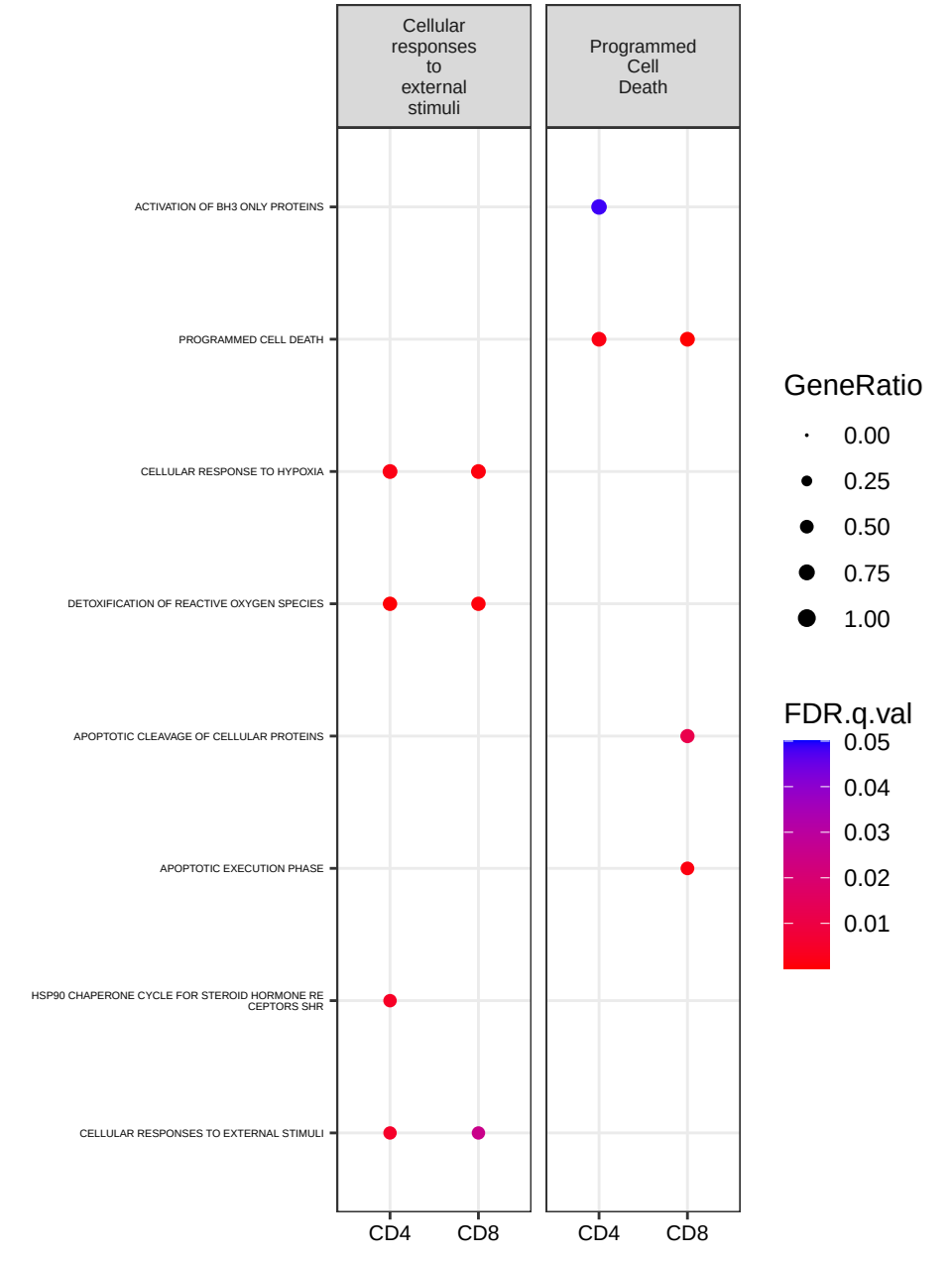
Cellular responses to external stimuli
Programmed Cell Death
ACTIVATION OF BH3 ONLY PROTEINS
PROGRAMMED CELL DEATH
CELLULAR RESPONSE TO HYPOXIA
DETOXIFICATION OF REACTIVE OXYGEN SPECIES
APOPTOTIC CLEAVAGE OF CELLULAR PROTEINS
APOPTOTIC EXECUTION PHASE
HSP90 CHAPERONE CYCLE FOR STEROID HORMONE RECEPTORS SHR
CELLULAR RESPONSES TO EXTERNAL STIMULI
CD4
CD8
CD4
CD8
GeneRatio
0.00
0.25
0.50
0.75
1.00
FDR.q.val
0.05
0.04
0.03
0.02
0.01

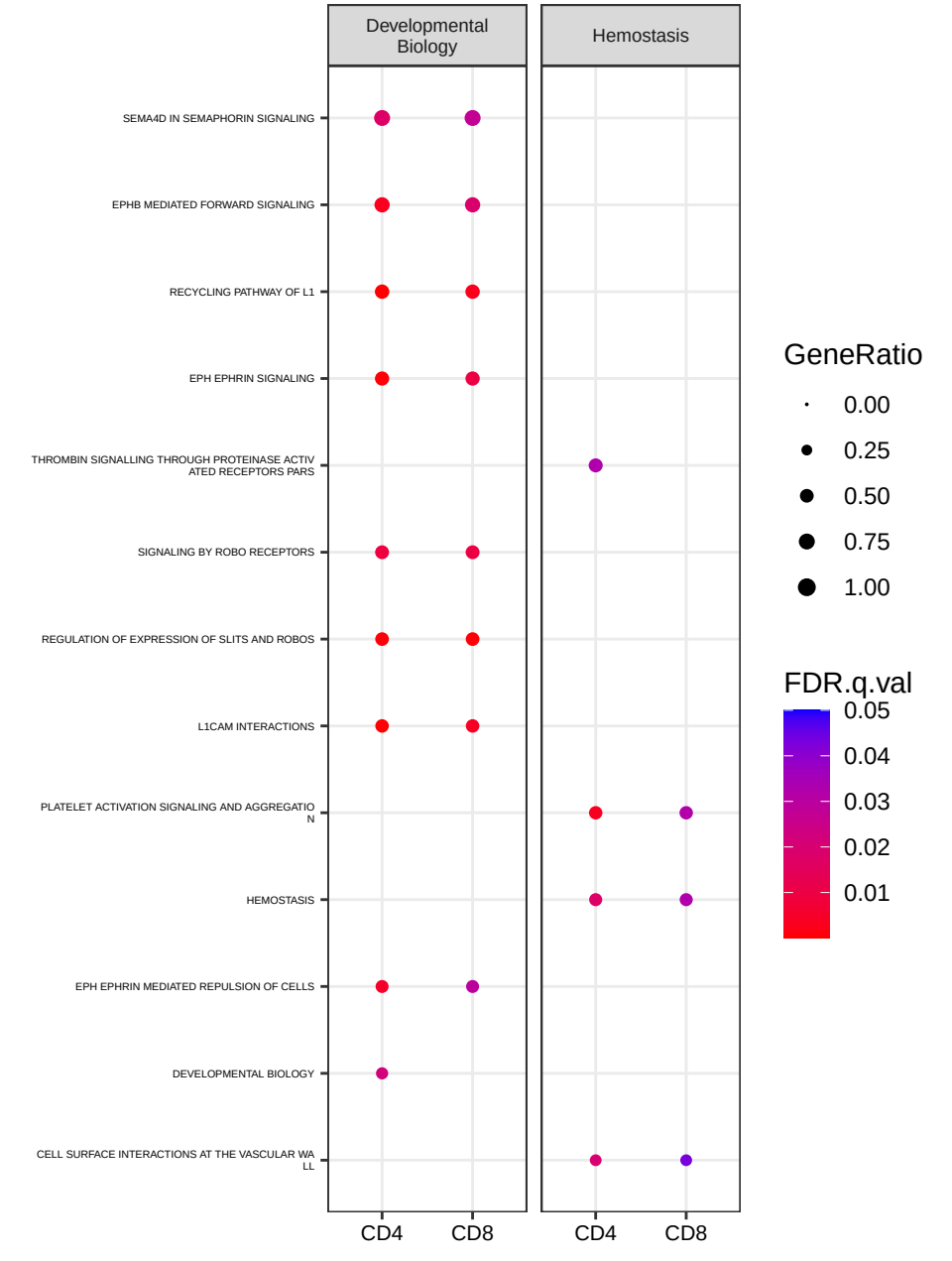
Developmental Biology
Hemostasis
SEMA4D IN SEMAPHORIN SIGNALING
EPHB MEDIATED FORWARD SIGNALING
RECYCLING PATHWAY OF L1
EPH EPHRIN SIGNALING
THROMBIN SIGNALLING THROUGH PROTEINASE ACTIVATED RECEPTORS PARS
SIGNALING BY ROBO RECEPTORS
REGULATION OF EXPRESSION OF SLITS AND ROBOS
L1CAM INTERACTIONS
PLATELET ACTIVATION SIGNALING AND AGGREGATION
HEMOSTASIS
EPH EPHRIN MEDIATED REPULSION OF CELLS
DEVELOPMENTAL BIOLOGY
CELL SURFACE INTERACTIONS AT THE VASCULAR WALL
CD4
CD8
CD4
CD8
GeneRatio
0.00
0.25
0.50
0.75
1.00
FDR.q.val
0.05
0.04
0.03
0.02
0.01

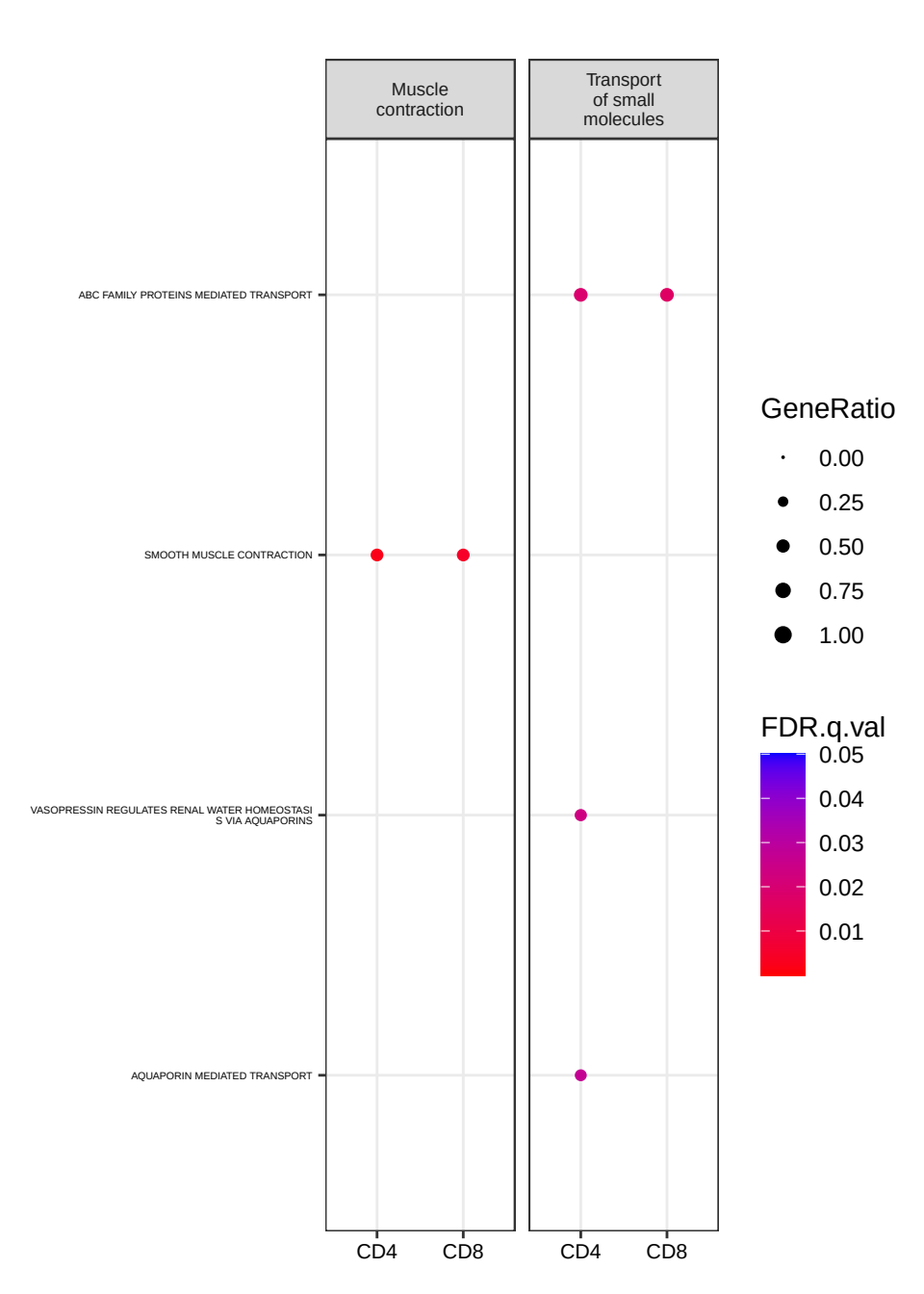
Muscle contraction
Transport of small molecules
ABC FAMILY PROTEINS MEDIATED TRANSPORT
SMOOTH MUSCLE CONTRACTION
VASOPRESSIN REGULATES RENAL WATER HOMEOSTASIS VIA AQUAPORINS
AQUAPORIN MEDIATED TRANSPORT
CD4
CD8
CD4
CD8
GeneRatio
0.00
0.25
0.50
0.75
1.00
FDR.q.val
0.05
0.04
0.03
0.02
0.01

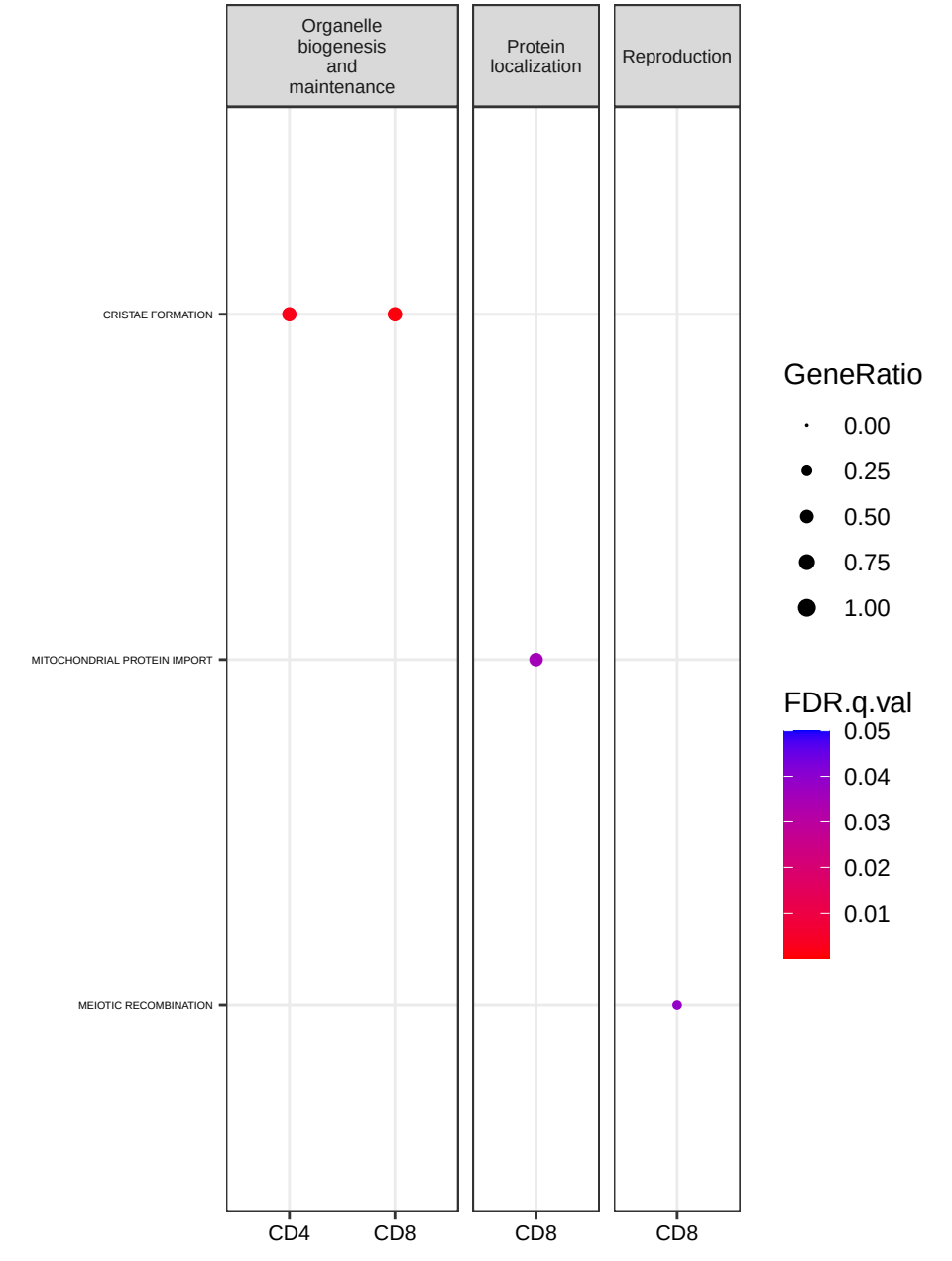
Organelle biogenesis and maintenance
Protein localization
Reproduction
CRISTAE FORMATION
MITOCHONDRIAL PROTEIN IMPORT
MEIOTIC RECOMBINATION
CD4
CD8
CD8
CD8
GeneRatio
0.00
0.25
0.50
0.75
1.00
FDR.q.val
0.05
0.04
0.03
0.02
0.01

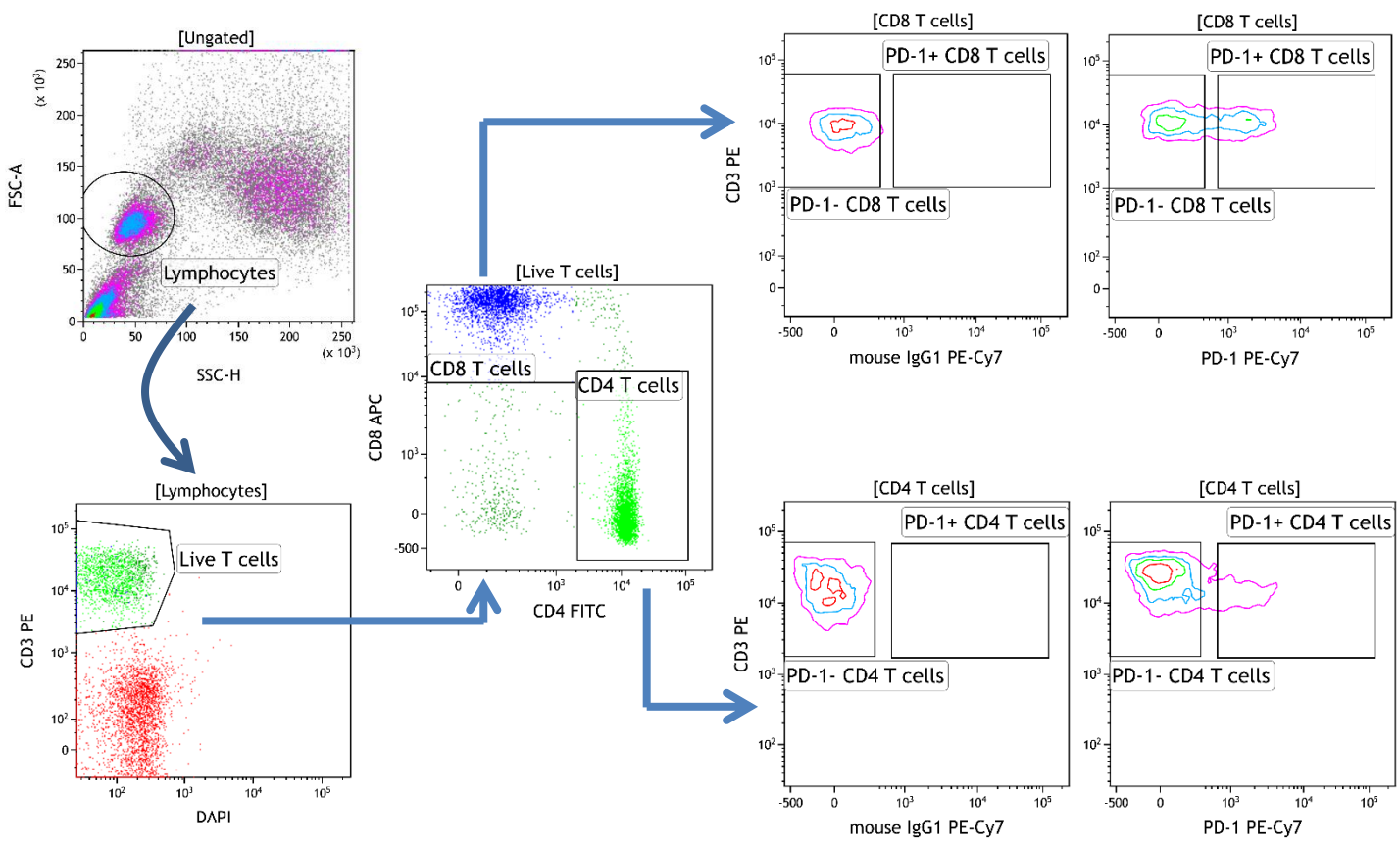

Supplemental Figure 1. Sorting strategy of T-cell subsets used for RNA sequencing. Mononuclear cells obtained after Ficoll density centrifugation were pelleted and incubated with a cocktail of anti-CD3/CD4/CD8/PD-1 antibodies, with 4',6-diamidino-2-phenylindole stain used to exclude dead cell. The following gating strategy was applied. $CD3^+$ $DAPI^-$ events (i.e. live T cells) were split in $CD4^+$ $CD8^-$ and $CD4^-$ $CD8^+$ populations and for both of them $PD\text{-}1^-$ and $PD\text{-}1^+$ cells were sorted. For each sample, $PD\text{-}1^-$ and $PD\text{-}1^+$ gates were adjusted before sorting with a negative control staining containing CD3/CD4/CD8 but an isotypic control instead of anti-PD-1 antibodies.

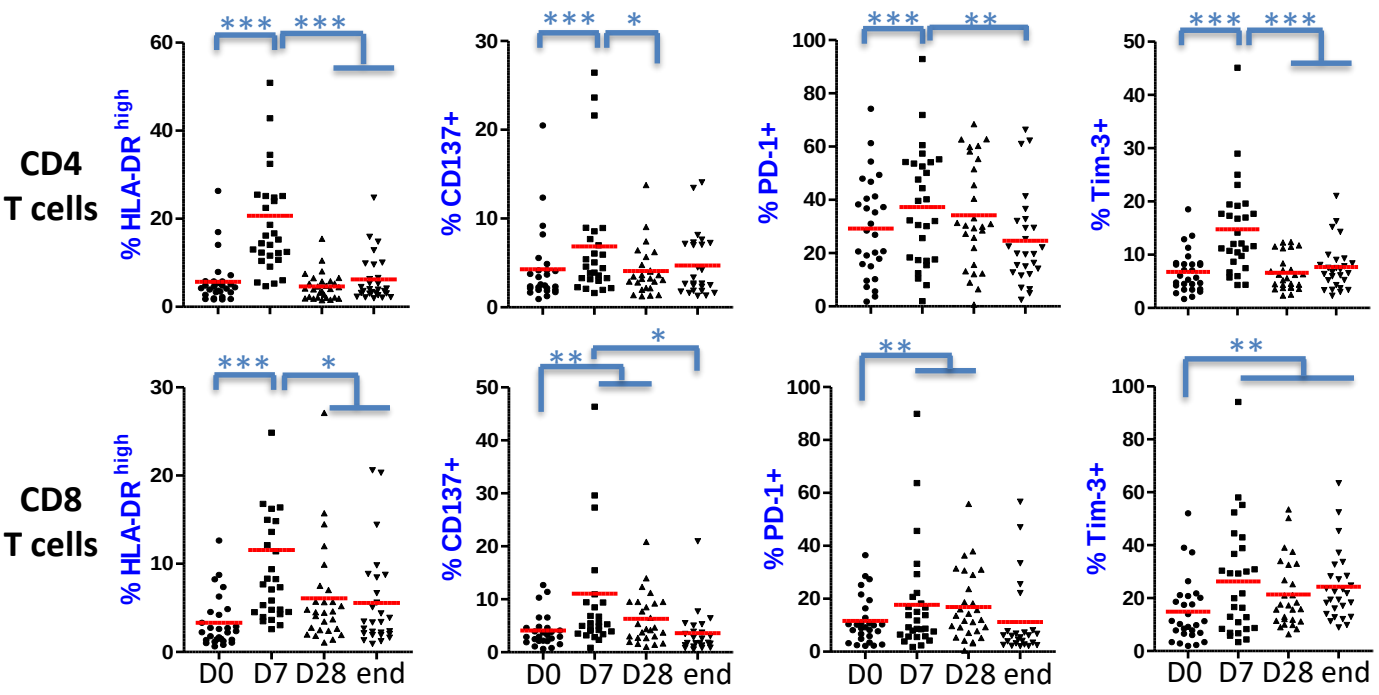

Supplemental Figure 2. Monitoring of HLA-DR, CD137, PD-1 and Tim-3 expression on circulating CD4 and CD8 T lymphocytes in GALEN R/R FL patients. Expression levels were measured by flow cytometry at the indicated time points. D0: 1st day of the 1st cycle of treatment (before lenalidomide intake); D7: 7th day of the 1st cycle (before obinutuzumab infusion); D28: 1st day of the 2nd cycle (before lenalidomide intake); end: end of induction. Median values are depicted as a red line. *p<.05, **p<.01, ***p<.001, multiple paired-samples Wilcoxon tests.

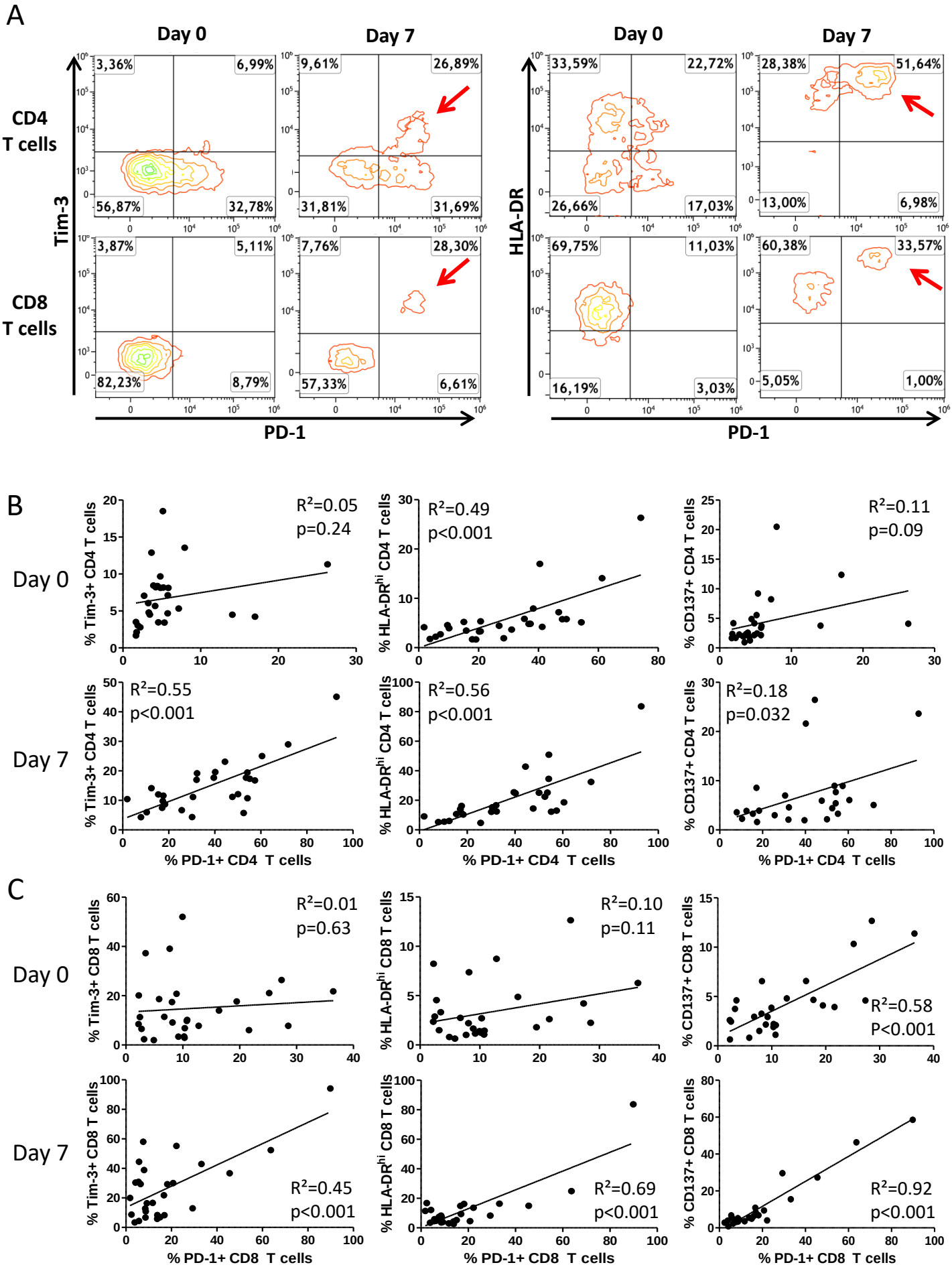
A
Day 0
Day 7
Day 0
Day 7
CD4 T cells
CD8 T cells
Tim-3
HLA-DR
PD-1
PD-1
3,36%
6,99%
56,87%
32,78%
9,61%
26,89%
31,81%
31,69%
3,87%
5,11%
82,23%
8,79%
7,76%
28,30%
57,33%
6,61%
33,59%
22,72%
26,66%
17,03%
28,38%
51,64%
13,00%
6,98%
69,75%
11,03%
16,19%
3,03%
60,38%
33,57%
5,05%
1,00%
B
Day 0
Day 7
% Tim-3+ CD4 T cells
% HLA-DRhi CD4 T cells
% CD137+ CD4 T cells
% PD-1+ CD4 T cells
R²=0.05
p=0.24
R²=0.49
p<0.001
R²=0.11
p=0.09
R²=0.55
p<0.001
R²=0.56
p<0.001
R²=0.18
p=0.032
C
Day 0
Day 7
% Tim-3+ CD8 T cells
% HLA-DRhi CD8 T cells
% CD137+ CD8 T cells
% PD-1+ CD8 T cells
R²=0.01
p=0.63
R²=0.10
p=0.11
R²=0.58
P<0.001
R²=0.45
p<0.001
R²=0.69
p<0.001
R²=0.92
p<0.001

Supplemental Figure 3. Correlation of PD-1 expression and activation/exhaustion markers. (A) Representative flow cytometry dot plots of PD-1 versus Tim-3 and PD-1 versus HLA-DR expression by CD4 (upper row) and CD8 T cells (bottom row) at D0 and D7. Red arrows indicate the PD-1^{+} Tim-3^{+} HLA-DR^{high} populations arising upon lenalidomide treatment (B) Correlations between PD-1 and Tim-3 expression (left panels), PD-1 and HLA-DR expression (middle panels), and PD-1 and CD137 expression (right panels) on CD4 T cells at D0 (upper row) and D7 (lower row) in R/R FL patients. (C) Correlations between PD-1 and Tim-3 expression (left panels), PD-1 and HLA-DR expression (middle panels), and PD-1 and CD137 expression (right panels) by CD8 T cells at D0 (upper row), and D7 (lower row) in R/R FL patients.

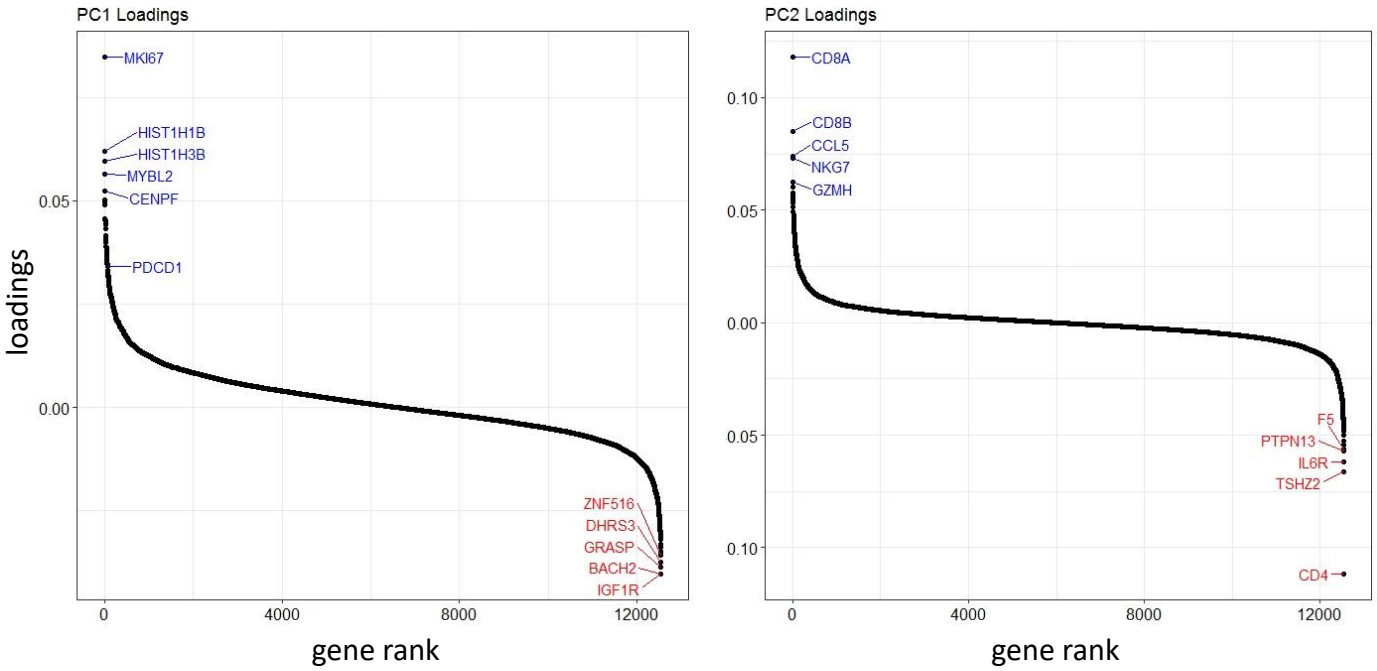

Supplemental Figure 4. Gene loadings on the two first principal components of the PCA (PC1 and PC2) depicted in Figure 2A**.** The loadings indicate how each gene contributes to a principal component. Loadings were ranked in decreasing order to emphasize the most contributive genes for each principal component. The top 5 genes were displayed, as well as PD-1 (PDCD1).

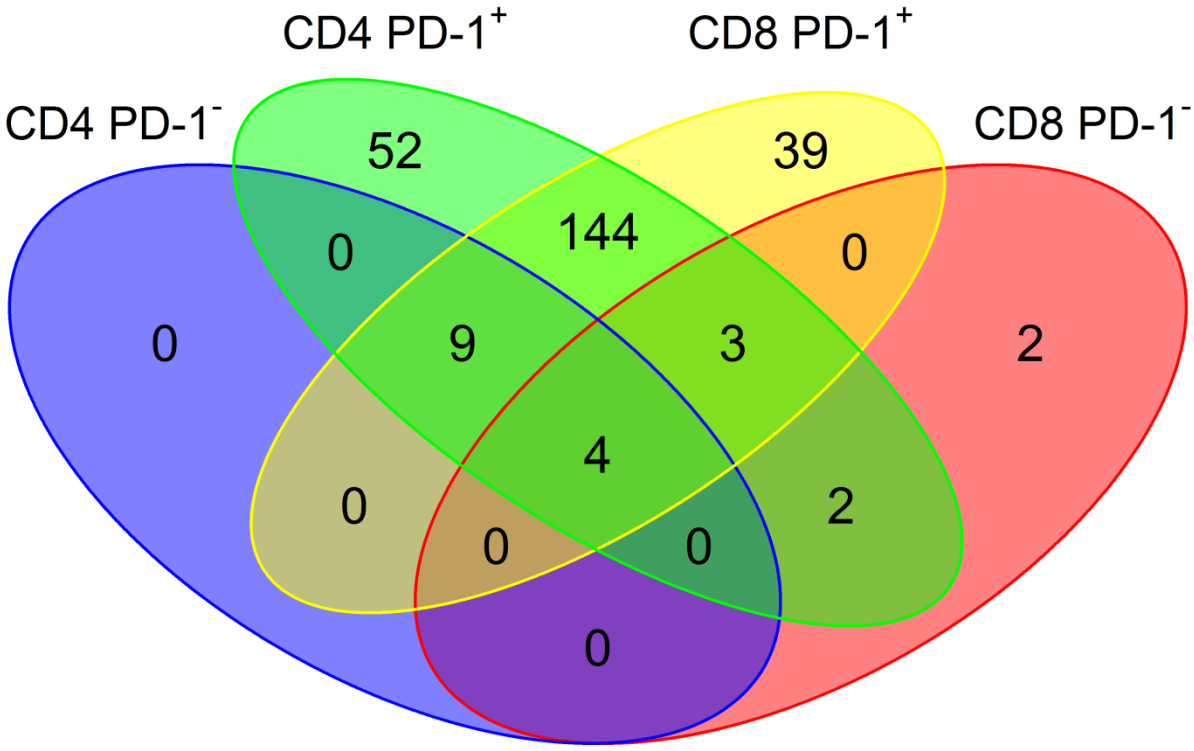

Supplemental Figure 5. Most biological processes triggered by lenalidomide are specific to PD-1$^+$ T cells. Venn diagram of pathways upregulated by lenalidomide in PD-1$^-$ CD4 T cells, PD-1$^+$ CD4 T cells, PD-1$^+$ CD8 T cells, and PD-1$^-$ CD8 T cells.

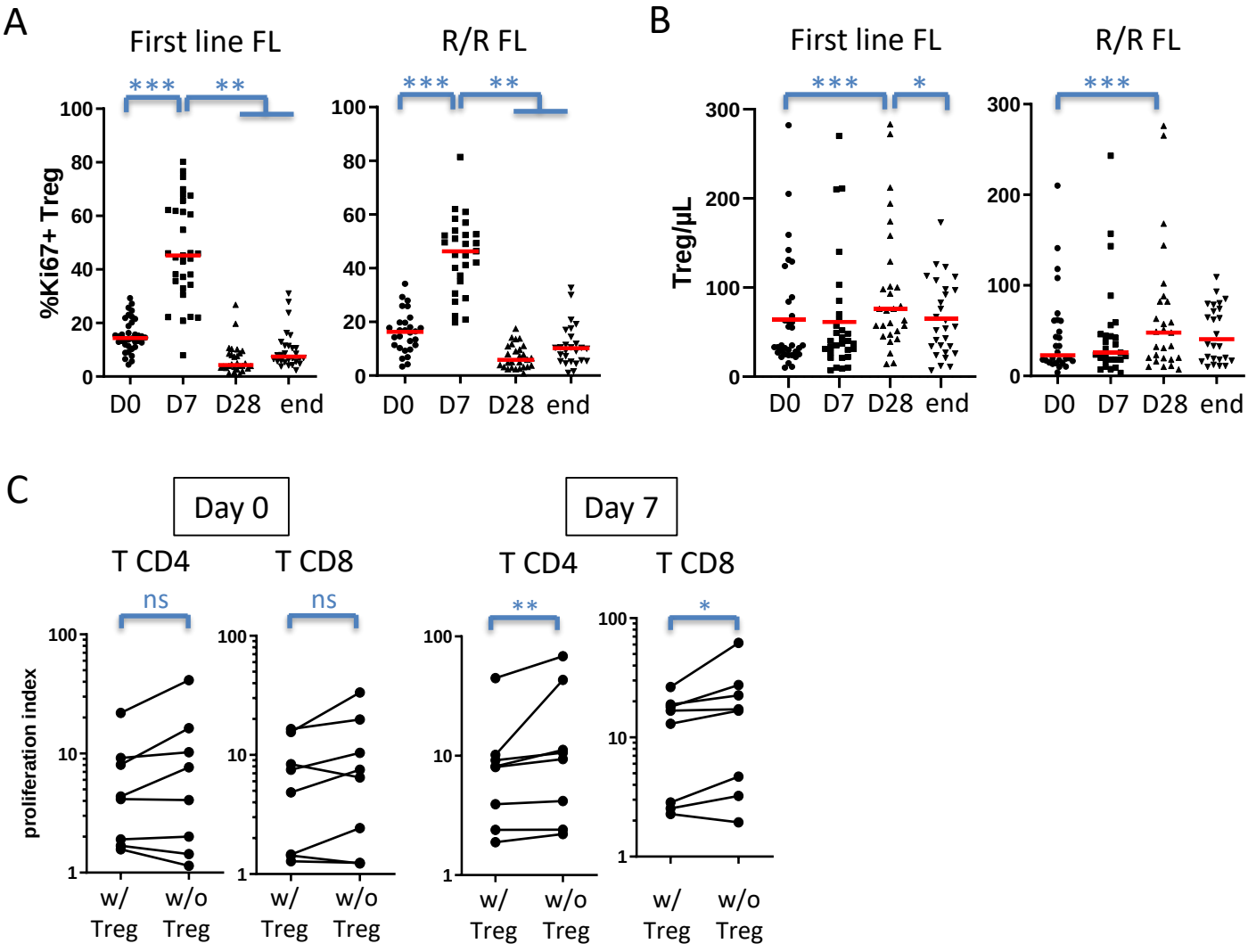

Supplemental Figure 6. Treg are not inhibited in vivo by lenalidomide. Ki-67 expression by blood Treg (A) and Treg cell count (B) determined by flow cytometry in first-line (left panel) and R/R (right panel) FL patients at indicated time points. D0: 1st day of the 1st cycle of treatment (before lenalidomide intake); D7: 7th day of the 1st cycle (before obinutuzumab infusion); D28: 1st day of the 2nd cycle (before lenalidomide intake); end: end of induction. Median values are depicted as a red line. (C) Proliferation index of CD4 and CD8 T cells stimulated ex vivo by CD3 and CD28 crosslinking before initiation (Day 0) and after one-week lenalidomide treatment (Day 7). PBMC (w/ Treg) were stimulated in parallel with Treg-depleted PBMC (w/o Treg) to indirectly evaluate Treg immunosuppressive activity. ns: not significant, *p<.05, **p<.01, ***p<.001, multiple paired-samples Wilcoxon tests

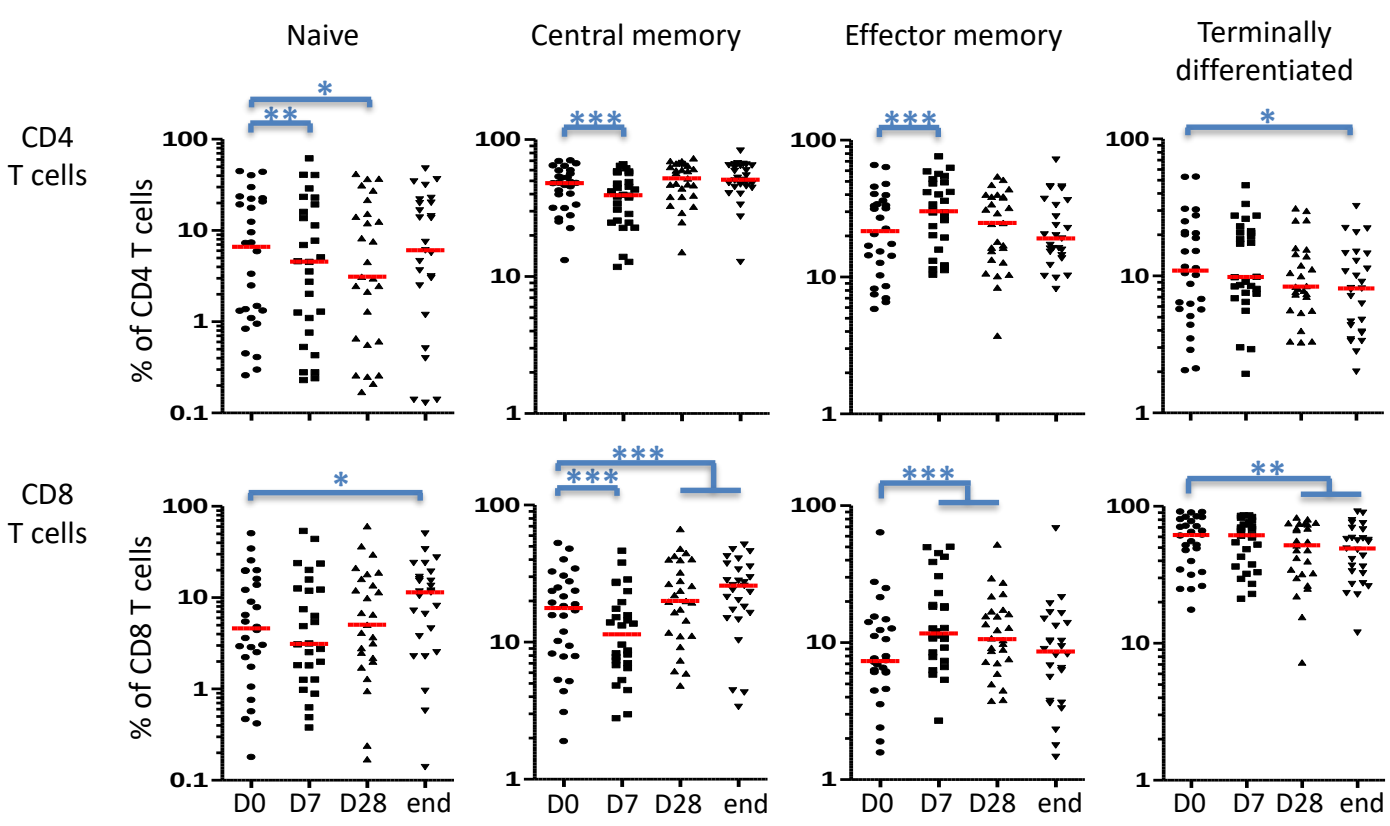

Supplemental Figure 7. Lenalidomide triggers an early shift of naïve and memory T-cell subsets in vivo in R/R FL patients. Percentages of naive, central memory, effector memory, and terminally differentiated effector T cells assessed by flow cytometry in circulating CD4 (upper row) and CD8 (lower row) T cells in R/R FL patients at the indicated time points. D0: 1st day of the 1st cycle of treatment (before lenalidomide intake); D7: 7th day of the 1st cycle (before obinutuzumab infusion); D28: 1st day of the 2nd cycle (before lenalidomide intake); end: end of induction. *p<.05, **p<.01, ***p<.001, multiple paired-samples Wilcoxon tests.

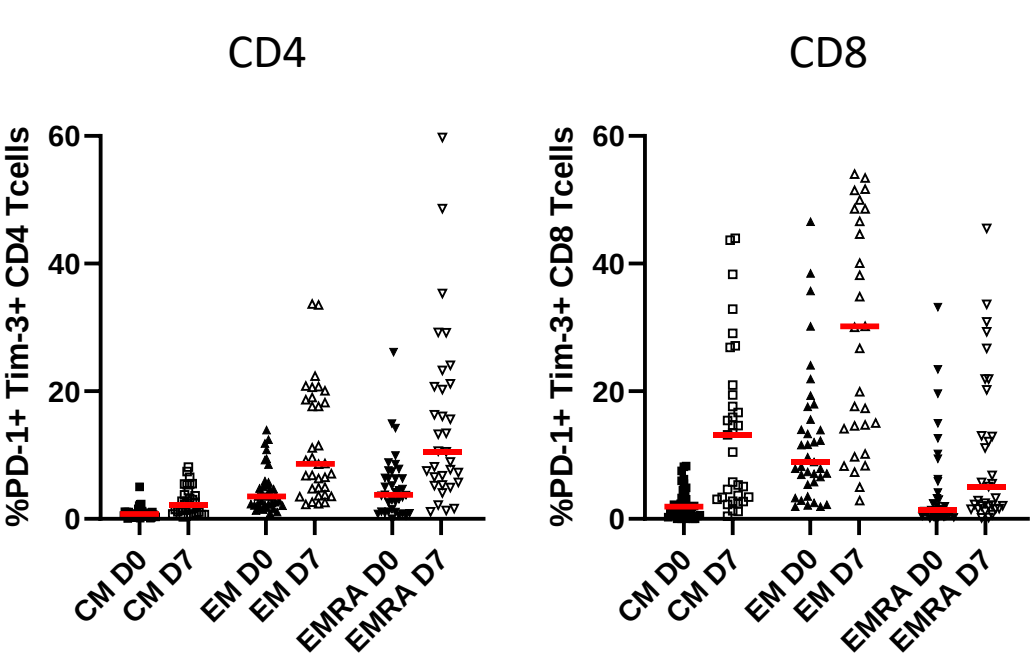

Supplemental Figure 8. Immune checkpoints co-expression is prominent in effector T cells. Percentages of PD-1 and Tim-3 co-expression in central memory (CM), effector memory (EM), and terminally differentiated effector (EMRA) T cells assessed by flow cytometry in circulating CD4 and CD8 T cells. D0: 1st day of the 1st cycle of treatment (before lenalidomide intake); D7: 7th day of the 1st cycle (before obinutuzumab infusion).

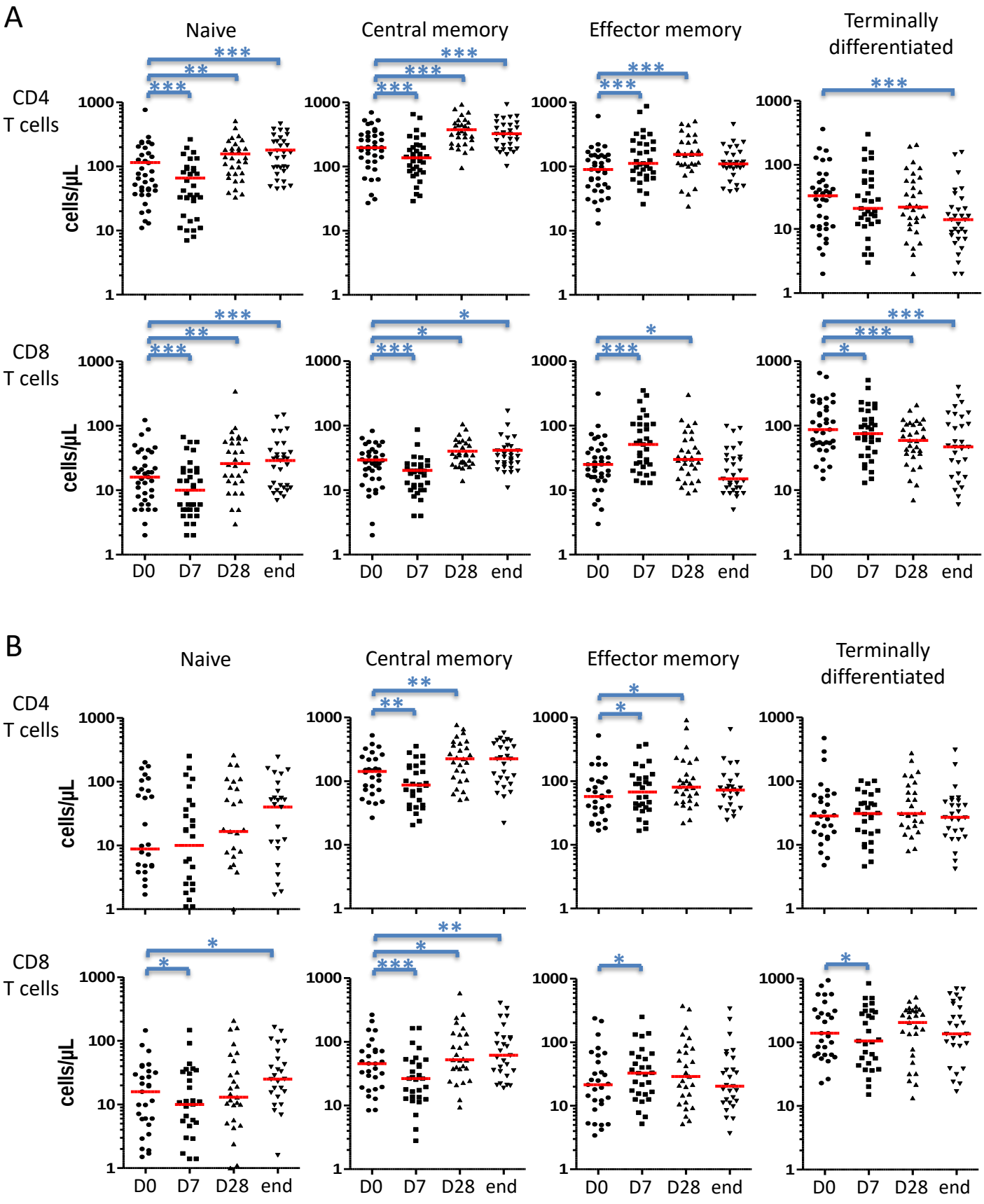
A
Naive
Central memory
Effector memory
Terminally differentiated
CD4 T cells
CD8 T cells
cells/µL
1000
100
10
1
***
**
*
D0
D7
D28
end
B
Naive
Central memory
Effector memory
Terminally differentiated
CD4 T cells
CD8 T cells
cells/µL
D0
D7
D28
end

Supplemental Figure 9. Lenalidomide increases effector memory T cells at the expanse of naive and central memory T cells in FL patients. Blood counts of naive, central memory, effector memory, and terminally differentiated effector T cells assessed by flow cytometry in circulating CD4 (upper row) and CD8 (lower row) T cells in first-line (A) and R/R FL patients (B) at the indicated time points. D0: 1st day of the 1st cycle of treatment (before lenalidomide intake); D7: 7th day of the 1st cycle (before obinutuzumab infusion); D28: 1st day of the 2nd cycle (before lenalidomide intake); end: end of induction. *p<.05, **p<.01, ***p<.001, multiple paired-samples Wilcoxon tests.

A

	% effector CD4 T cells		% Treg in CD4 T cells	
	Hazard ratio	Cox p value	Hazard ratio	Cox p value
Day 0	1.51	0.016	3.55	0.005
Day 7	1.08	0.014	1.023	0.0004
D28	1.75	0.008	1.07	0.05
End of induction	1.08	0.014	2.54	0.003

B

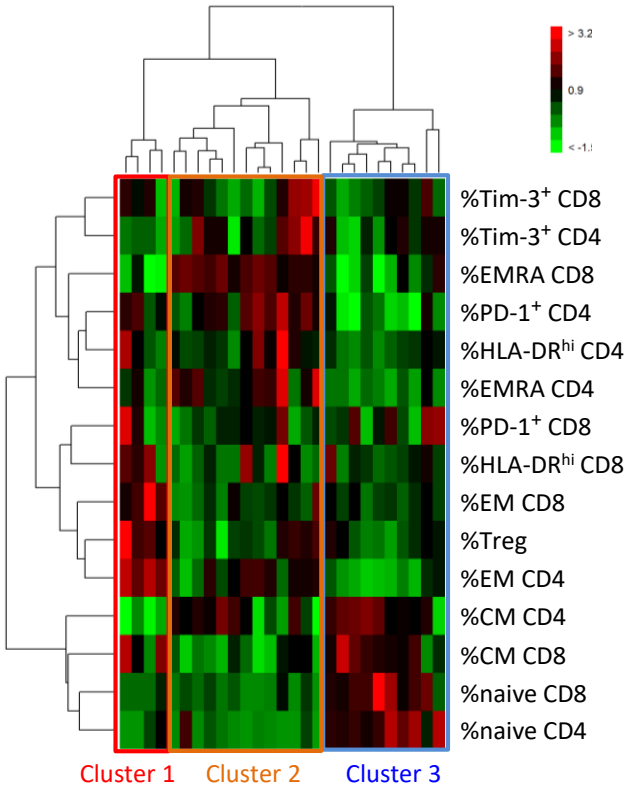

C

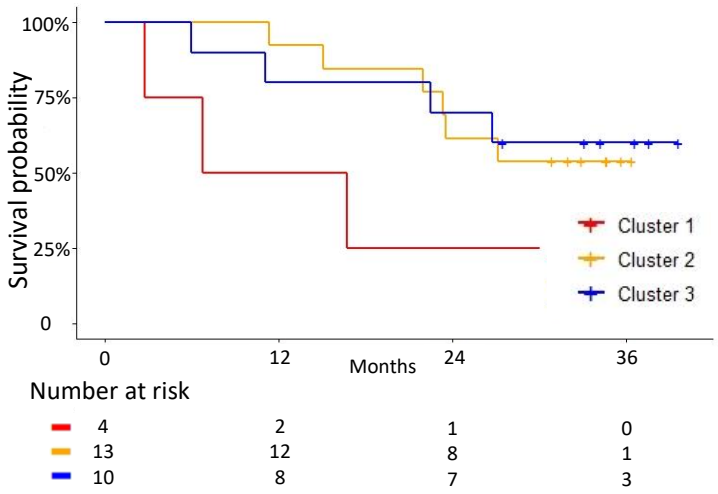

Supplemental Figure 10. Blood T-cell immunophenotyping at presentation pinpoints an unfavorable profile in FL patients treated with lenalidomide to obinutuzumab combination. (A) Summary table of prognostic values of effector CD4 T cells and Treg percentages at the 4 sampling time points (univariate Cox model). D0: 1st day of the 1st cycle of treatment (before lenalidomide intake); D7: 7th day of the 1st cycle (before obinutuzumab infusion); D28: 1st day of the 2nd cycle (before lenalidomide intake) (B) Unsupervised hierarchical clustering of the 27 R/R patients in 3 groups based on 15 immune parameters. Treg: regulatory CD4 T cells, CM: central memory, EM: effector memory, EMRA: terminally differentiated effector T cell. (C) Progression-free survival curves of the 3 patient clusters.